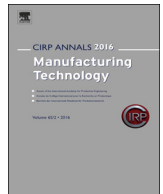




Contents lists available at ScienceDirect

CIRP Annals - Manufacturing Technology

journal homepage: <http://ees.elsevier.com/cirp/default.asp>

On the influence of gamma prime upon machining of advanced nickel based superalloy

Zhirong Liao^a, Dragos Axinte (1)^{a,*}, Maxime Mieszala^b, Rachid M'Saoubi (1)^c, Ali Abelhafeez^a, Johann Michler^b, Mark Hardy^d

^aRolls-Royce UTC in Manufacturing and On-Wing Technology, Faculty of Engineering, University of Nottingham, UK

^bEMPA, Swiss Federal Laboratories for Materials Testing and Research, Laboratory for Mechanics of Materials and Nanostructures, Thun, Switzerland

^cSeco Tools AB, R&D Material and Technology Development, Fagersta, Sweden

^dRolls-Royce plc, Derby, UK

ARTICLE INFO

Keywords:
Nickel Alloy
Machining
Gamma prime phase

ABSTRACT

Whilst gamma prime (γ') phase is the strengthening phase in Ni-based superalloys its influence on machining has been seldom investigated. This paper reports for the first time on the effect of γ' upon machining of Ni-based superalloys when cutting with parameters yielding different cutting temperature intervals which lead to strengthening/softening effects on the workpiece (sub) surface. In-depth XRD, SEM/FIB, EBSD analysis and unique micro-pillar testing in the workpiece superficial layers indicated that with the increase of γ' fraction the grain plastic deformation significantly decreased, while specific cutting energy can switch from low to high values influenced by the real cutting temperature.

© 2018 Published by Elsevier Ltd on behalf of CIRP.

1. Introduction

With the microstructure consisting of γ matrix and γ' precipitating and strengthening phase, Ni-based superalloys are widely used for the manufacture of safety critical components of aeroengines due to their high strength at elevated temperatures. This high performance is due to the significant volume fraction of γ' phase that stops the penetration of dislocations from γ constituent with its ordered L12 structure [1]. Thus, the development of these Ni-based superalloys is oriented towards high volume fractions of γ' (e.g. from ca. 25% of first generation to 60% for recent alloys respectively) to reach a set of optimum of mechanical properties (i.e. strength under high temperature) [2]. However, with the increase of γ' fraction, these alloys could display fast crack growth rates, which is an undesired effect. Consequently, when developing Ni-based superalloys for safety-critical applications, it is beneficial to achieve the desired strength performance with the minimum required volume fraction of γ' [3].

On the other hand, the machining defects (e.g. white layer, grain plastic deformation) are important factors that could influence the failure of the parts made of Ni-based superalloys [4–6]. However, the precipitation strengthening effect, which enhances the material tolerance to surface damage during machining, is only effective under a certain temperature range that when exceeded, can induce more material thermal softening thus inducing severer machining defects. This temperature range is highly dependent on the proportions of γ' (Fig. 1 [7]), where a high volume fraction of γ' yields a higher temperature range of strengthening effect. While this dependency is exploited by material developers, limited

information exists on the effect of γ' volume fraction upon workpiece surface integrity at microscopic level when machining.

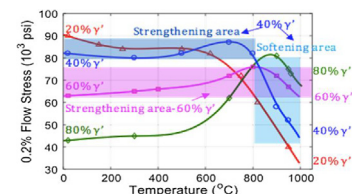


Fig. 1. Variation of the flow stress of Ni-based alloys with temperature for various proportions of γ' [7].

In this respect, this paper investigates for the first time on the influence of the γ' phase proportion upon the machinability and surface integrity of Ni-based superalloys. Due to the small range of the affected layer depth on the machined subsurface, e.g. grain deformation and recrystallizations, which are around/under tens of micrometres, advanced material investigation methodology, i.e. in-depth X-Ray diffraction (XRD), scanning electron microscope (SEM), focused ion beam (FIB), Electron backscatter diffraction (EBSD) analysis and state-of-the-art micro-pillar testing were employed to understand the phenomena governing the material microstructural evolution during the machining process.

2. Experimental approach and methodology

In this study, two Ni-based superalloys consisting of similar chemical composition (Table 1) but with different volume fraction of γ' (43% γ' and 57% γ' for alloys A and B, respectively) were investigated to enable the understanding of the influence of γ' phase upon the machining process. Powder compacts, about

* Corresponding author.

E-mail address: Dragos.Axinte@nottingham.ac.uk (D. Axinte).

76 mm in diameter with can, were produced by hot isostatic pressing and heat treated to produce a fine grain microstructure.

Table 1

Chemical composition of the two Ni-based superalloys (wt%).

	No.	Ni	Cr	Co	C	Mo	Zr	Nb	Ta	Al	Ti	B	Hf	W	Fe	Mn
A	Bal.	15	18.5	0.03	5	0.06	0	2	3	3.6	0.02	0.5	0.01	0.03	0	
B	Bal.	12.3	4.0	0.03	0.6	0.06	2.1	4.6	3.8	2.6	0.02	0	3.1	3.4	0.5	

Using advanced ion contrast channelling imaging it was revealed, both grain orientation and γ/γ' phase microstructure without chemical etching (Fig. 2). Similar grain size could be easily observed of these two different alloys while Alloy B shows more γ' phase under the high γ/γ' contrast imaging.

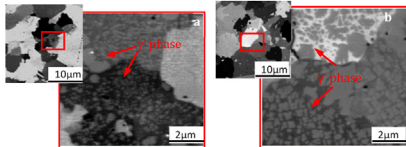


Fig. 2. Microstructure of (a) Alloy A (43% γ') and (b) B (57% γ') by advanced ion contrast channelling imaging.

Plunge turning were performed in orthogonal cutting mode using custom made Seco inserts ($\gamma = 0^\circ$, $\alpha = 7^\circ$, 10 μm edge radius) to study the machinability and surface integrity of these two alloys. Two cutting conditions yielding different cutting temperatures were used: (i) "normal conditions" with new tool and cutting speed $v_c = 30$ m/min, feed rate $f = 0.1$ mm/rev; (ii) "aggressive conditions" with worn ($VB = 0.3$ mm) tool, $v_c = 80$ m/min, $f = 0.1$ mm/rev. An infrared CCD thermal camera was employed to measure the cutting temperature focusing on the cutting edge while dry cutting condition was employed to allow the temperature measurement.

The machined (sub) surface was studied with SEM following electrolytic etching with orthophosphoric acid. EBSD was also applied with scanning step size of 0.5 μm for deformed grain area and 0.05 μm for recrystallized layer. A Proto XRD diffractometer was employed to measure the residual stress under the machined surface. To test the material strength within the machined subsurface, an advanced micro-pillar compression test (Alemnis) was applied in both the bulk material and machined edge.

3. Machinability investigation of two different alloys

3.1. Cutting temperature

Under normal cutting conditions both alloys yield similar cutting temperatures (max. 750 $^\circ\text{C}$) at the tool tip-workpiece contact area while under aggressive cutting condition it reached max. 950 $^\circ\text{C}$ (Fig. 3). Due to the temperature dependence of γ' properties (Fig. 1), the flow stress of these two alloys yielded different strengthening/softening effects correspondingly. For Alloy A (43% γ'), within normal cutting condition the max. cutting temperature (750 $^\circ\text{C}$) is still in the strengthening effect zone (Fig. 1), while the material is softened significantly during aggressive cutting where the maximum cutting temperature reached 950 $^\circ\text{C}$. However, at this cutting temperature zone (700–950 $^\circ\text{C}$) Alloy B (57% γ') is mainly under strengthening condition, which is around the peak point of the stress while the softening effect could be neglected. Thus, in aggressive cutting conditions, although similar temperature is achieved, the Alloy A and B are in totally different strength status.

3.2. Specific cutting energy

The specific cutting energy (SCE), Eq. (1) [8,9], for which cutting temperature is an indicator, could be used to evaluate the

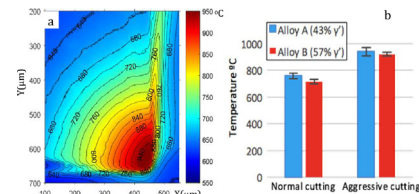


Fig. 3. (a) Example of temperature map (aggressive cutting) and (b) max. cutting temperatures at the tool-workpiece interface (error bars – 1Stdev).

machinability of these two alloys:

$$E = E_s + E_f + E_p = \frac{F_s}{A_s} \frac{\cos\gamma}{\sin\phi\cos(\phi-\gamma)} + \frac{F_n\sin\gamma + F_c\cos\gamma}{bh_c} + \frac{F_pV_s}{hfV_c} \quad (1)$$

where: E , E_s , E_f , E_p – total, shear, friction and ploughing specific energy; F_s , F_c , F_n , F_p – shearing, cutting, normal cutting and ploughing force; ϕ – shear angle; A_s and V_s – shear area and cutting speed; b , h and h_c – cutting width, undeformed and deformed chip thickness; these parameters can be measured or calculated [8,9].

As shown in Fig. 4, the SCE mainly stems from the contribution of friction and shear energy while the ploughing energy is low compared with others due to applied small edge hone. Under normal cutting condition, the SCE of Alloy A (43% γ') is similar to Alloy B (57% γ'). This is because under these conditions the cutting temperature of both alloys is max. 750 $^\circ\text{C}$ where both alloys are under strengthening effect (region <800 $^\circ\text{C}$ – Fig. 1).

Under aggressive cutting conditions, it is interesting to see the specific friction energies (SFE) of both alloys are similar while the specific shear (SSE) and total energy of Alloy A (43% γ') are much lower than Alloy B (57% γ'). This is because under high cutting temperature (region >800 $^\circ\text{C}$ – Fig. 1) the material flow stress of Alloy A is reduced due to softening effect while Alloy B is still in strengthening condition, leading to higher SSE while SFE is the same since both friction coefficients did not change significantly.

Observing the influence on cutting temperature and specific machining energy from the volume fractions changes of γ' , it can be expected that the surface integrity of machined workpiece will be affected significantly. This leads to the need of study on the microstructural phenomena occurring at micrometric level.

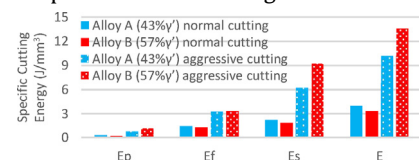


Fig. 4. Specific energies of two alloys under different cutting conditions.

4. Surface integrity impact from the changing of γ' phase

4.1. Metallographic study

Fig. 5a, b shows SEM images of machined subsurface in normal cutting conditions where both alloys present similar level of material drag (ca. 6 μm) while in aggressive cutting conditions (Fig. 5c, d) they display comparable (ca. 4 μm) level of recrystallized layer (white layer). However, it is surprising to find in aggressive cutting condition that Alloy A shows higher level of material drag under the white layer while Alloy B shows nearly no material drag under this condition. This is because at normal cutting condition both alloys were under the temperature zone yielding material strengthening which leads to similar level of material drag. On the other hand, under aggressive machining condition high cutting temperature (950 $^\circ\text{C}$) was reached, where the Alloy A shows softening effect due to lower γ' fraction, while Alloy B was still under strengthening stage because of higher γ' fraction. Thus, although the recrystallization occurred in both

Download English Version:

<https://daneshyari.com/en/article/8038652>

Download Persian Version:

<https://daneshyari.com/article/8038652>

[Daneshyari.com](https://daneshyari.com)